An Analysis of Climatological Patterns of the Northern Hemispheric Circulation[1,2]

THOMAS R. HEDDINGHAUS

Climatic Analysis Center, National Meteorological Center, National Weather Service/NOAA, Washington, DC 20233

ERNEST C. KUNG

Department of Atmospheric Science, University of Missouri, Columbia, MO 65211

(Manuscript received 30 March 1979, in final form 1 October 1979)

ABSTRACT

Eigenvector and harmonic analyses have been performed with monthly mean values of upper air parameters of the Northern Hemispheric circulation for the period from April 1955 to December 1974. The parameters used involve the 700 and 500 mb temperatures, the 700–500 mb thickness, the 300 mb kinetic and eddy kinetic energies, and the 700, 500 and 300 mb zonal/meridional flow indicators. The zonal/meridional flow indicator is defined as the ratio $|\overline{u}|/|\overline{v}|$, where the bar indicates the monthly mean.

The first eigenvectors of the normalized parameters are associated with the annual variation of the basic patterns. For the temperature field the first eigenvector overwhelmingly dominates. It reflects the annual variation of temperature in the mid and higher latitudes with an effect of the land-ocean configuration. The second eigenvector shows a land-ocean contrast. The long-term variation of temperature in the lower latitudes also stands out. For the kinetic energy and zonal/meridional flow indicator the first eigenvectors are not as dominant as that of temperature. They reflect the subtropical jet and other hemispherical-scale circulations. The third eigenvector of kinetic energy and second eigenvector of the zonal/meridional flow indicator appear to be associated with the semiannual oscillations of the large-scale wind systems including summer and winter monsoons. It also appears that high-numbered eigenvectors of kinetic energy and zonal/meridional flow indicators are associated with long-term variations in the lower latitudes and short-term variations in the mid to high latitudes.

1. Introduction

The utility of eigenvector analysis to describe the important modes of variance has been demonstrated by various authors in climatic studies of surface observations. It is the purpose of this paper to present the observed climatological patterns of selected upper air parameters in the Northern Hemisphere through the application of eigenvector and harmonic analyses.

Kutzbach (1967) used eigenvector analysis to study the large-scale features of monthly pressure, temperature and precipitation patterns over North America. In a related paper, Kutzbach (1970) also examined sea level pressure patterns over the Northern Hemisphere. A study of monthly means of surface pressure, temperature and rainfall over both hemispheres and the tropical belt was made by Kidson (1975a,b). His approach differed from that of Kutzbach in that the continuous time series were used for a period of 10 years, whereas Kutzbach utilized long-term series of specific time or month of the year. In his study of a quasi-biennial standing wave, Trenberth (1975) performed an empirical orthogonal function analysis of monthly mean sea surface pressure deviations in the Australian area and monthly mean sea surface temperature anomalies in the Tasman Sea. Weare (1977) also published a similar analysis on seasonal sea surface temperatures in the Atlantic Ocean. Eigenvector analysis of the daily 500 mb geopotential topography over the Northern Hemisphere was made by Craddock and Flood (1969), and Rinne (1971) studied the forecasting errors of a simple barotropic model at the 500 mb level with the aid of empirical orthogonal functions.

The present study is based on 20 and 17 years of Northern Hemispheric monthly mean values for temperature, kinetic energy, and a circulation index at the 700, 500 and 300 mb levels. Our aim is to present the spatial variations and associated temporal variations of the important mutually independent components of the variables. These components are the eigenvectors which explain the major portion of variance in the data and could be viewed as representative of basic climatological patterns of the Northern Hemispheric circulation.

[1] Research supported by the Climate Dynamics Research Section, National Science Foundation.

[2] Contribution from The Missouri Agricultural Experiment Station, Journal Series No. 8342.

0027-0644/80/010001-17$08.25

2. Data and scheme analysis

The data used in this study were processed from the National Meteorological Center (NMC) octagonal grid data at 1977 points over the Northern Hemisphere, which were obtained from the National Center for Atmospheric Research. The set contained daily 1200 GMT temperature and geopotential height values at the 700, 500 and 300 mb pressure levels for a period from April 1955 through December 1974. This set of data had a missing portion from 1958 to 1962 and was filled in by a separate data set which had been processed from daily 0000 GMT aerological observations at 704 stations in the Northern Hemisphere. This observational data set was originally obtained from the MIT General Circulation Data Library and later re-edited at the University of Missouri-Columbia (see Kung, 1977).

To prepare the input data for climatological analysis a rectangular grid system of 12 × 12 points over the Northern Hemisphere was specified with grid points at every 5° of latitude and 30° of longitude from 15 to 70°N inclusive. Daily values of the geostrophic wind components were first computed for all interior points in the NMC octagonal grid system as a reasonable approximation to the upper air wind. The temperature, height and geostrophic wind components at the NMC octagonal grid points were then interpolated to the rectangular grid points by using a distance-weighted average of the four closest NMC octagonal grid points with a weighting function, which was modified from what had been originally given by Cressman (1959). The weighting function is given by

$$W = 1/(d + 0.5)^2,$$

where d is the angular distance in degrees along an arc in the great circle between the octagonal and rectangular grid points. The constant 0.5 was inserted to prevent the weighting function from becoming too large for very small values of d. The MIT data set of station values was interpolated at rectangular grids in a similar manner by using the distance weighted average of the 15 closest stations. The geostrophic wind components were then computed at the rectangular grids for the MIT data set. A comparison of monthly averages of the two data sets at rectangular grid points for four months in 1963 when the data periods overlapped showed good agreement between the two sets.

Examples of the Northern Hemispheric station network are found in several sources (e.g., Oort and Rasmusson, 1971; Gray *et al.*, 1976). A scarcity of stations in the south-central Atlantic and southeastern Pacific may be readily noticed in the aerological network. Although the input data in this study were those interpolated at the rectangular grid points either indirectly from NMC grid data or directly from the observed values, the general problem associated with the data scarcity in these areas is also inherent in this study. Thus some reservations of the results as presented in this paper for these areas may be necessary.

The temperature, geopotential height and wind components at rectangular grids were utilized to compute various monthly values for further analysis. These monthly mean parameters include the temperature at 700 and 500 mb, the 700–500 mb thickness, the kinetic energy and eddy kinetic energy, and the "zonal/meridional flow indicator" $\overline{|u|}/\overline{|v|}$ at 700, 500 and 300 mb, where u and v are eastward and northward geostrophic wind components and the bar indicates the monthly mean. The kinetic energy is defined for a 50 mb pressure layer by $k = \frac{1}{2}(u^2 + v^2)$ and the eddy kinetic energy by $k_e = \frac{1}{2}(u'^2 + v'^2)$, where u' and v' are the perturbations of u and v from the respective zonal means. As the original data set starts in April 1955, the months of January, February and March 1955 were supplemented utilizing multiannual monthly mean values in order to complete a 20-year period for the parameters at the 500 and 700 mb levels. For the parameters at the 300 mb level the time series were constructed with 17 years of data because of limited availability during the early period, omitting the period from 1955 to 1957.

Each of the parameters used in the study is indicative of a certain climatological characteristic of the large-scale circulation. The 700 mb temperature and the 700–500 mb thickness are considered to be associated with the degree of surface heating. The 500 mb temperature is analyzed to study its relationship with the 700 mb temperature field. The 300 mb kinetic and eddy kinetic energies are measures of the strength of the circulation in the upper troposphere. The ratio $\overline{|u|}/\overline{|v|}$ which is defined as the zonal/meridional flow indicator in this study should not be confused with the zonal index which is customarily referred to as the hemispherically averaged zonal wind component or horizontal pressure difference between 35 and 55° latitudes (see Wahl, 1972). An eddy term $\overline{u'v'}$ may also have a relevance as a measurement of the strength of the meridional flow since it is a correlation term to measure the momentum transport. However, in this study the ratio $\overline{|u|}/\overline{|v|}$ is taken to directly compare these two components of the motion. The 300 mb $\overline{|u|}/\overline{|v|}$ ratio measures the strength of the zonal flow relative to the meridional flow in the upper troposphere. A low value of this ratio would indicate meridional type of flow patterns during the month and a consequent dominance of severe or "anomalous" weather conditions. The 700 and 500 mb $\overline{|u|}/\overline{|v|}$ ratios are analyzed for comparison with the 300 mb zonal/meridional flow indicator.

The problem of determining the eigenvector patterns of meteorological variables can be handled in different ways depending on the nature of the

TABLE 1. Percentage variance of the first 10 eigenvectors for various normalized parameters.

Parameter	Eigenvector										
	1	2	3	4	5	6	7	8	9	10	Total
700 mb temperature	82.4	3.5	2.9	1.4	1.2	0.9	0.7	0.6	0.6	0.5	94.7
500 mb temperature	81.5	4.8	2.1	1.5	1.2	1.0	0.8	0.7	0.6	0.5	94.7
700–500 mb thickness	80.9	4.8	2.3	1.4	1.2	1.0	0.7	0.7	0.6	0.5	94.1
300 mb kinetic energy	34.7	9.5	6.1	4.9	4.3	3.4	3.0	2.8	2.6	2.1	73.4
300 mb eddy kinetic energy	42.9	6.5	4.7	3.7	3.4	3.0	2.4	2.1	1.7	1.6	72.0
700 mb zonal/meridional flow indicator	14.1	7.1	6.3	4.7	4.4	3.7	3.5	3.1	2.7	2.4	52.0
500 mb zonal/meridional flow indicator	19.6	6.9	6.6	4.9	4.3	3.7	3.5	3.0	2.7	2.6	57.8
300 mb zonal/meridional flow indicator	22.1	7.1	6.2	4.9	4.4	4.0	3.5	3.0	2.9	2.6	60.7

time series employed (see Kutzbach, 1967; Stidd, 1967; Kidson, 1975a,b). Following the method as described by Kidson an eigenvector analysis is performed on time series of the monthly mean parameters at rectangular grids. The time series are normalized for eigenvector analysis by subtracting the total time mean at each rectangular grid point from the monthly mean values and then dividing the differences by the corresponding standard deviation of the time series. This was done so that the eigenvector patterns would not be dominated by the extreme variation of the parameter at different locations. The number of grid points used is 144 for all eight parameters and the number of months is 240 (20 years) for parameters at the 700 and 500 mb levels and 204 (17 years) for the parameters at the 300 mb level.

Harmonics are also determined for the monthly mean values of parameters over the corresponding periods of monthly values at all 144 grid points in accordance with the manner described by Kung and Soong (1969). Utilizing the result of the harmonic analysis the fractional variance may then be calculated as described by Kung and Soong. The fractional variance Q_n indicates the percentage contribution of the nth harmonic to the total variance, and is defined as $Q_n = (C_n^2/2S^2) \times 100$, where C_n is the amplitude of the nth harmonic and S^2 the total variance.

3. Eigenvector components

The percentage of variance explained by the first 10 eigenvectors and their sum for each normalized parameter is shown in Table 1. The sum of the 10 largest eigenvectors explains more than 94% of the variance for the 700 and 500 mb temperatures and 700–500 mb thickness, over 72% for the kinetic and eddy kinetic energies at 300 mb, and 52–61% for the zonal/meridional flow indicators $\overline{|u|}/\overline{|v|}$ at 700, 500 and 300 mb. This compares favorably with Kidson's (1975a) results with 10 years Northern Hemispheric monthly mean data of surface temperature and pressure, which are 98.6 and 91.7%, respectively, for the first 10 components. A favorable comparison may also be made with results of Craddock and Flood (1969) with daily 500 mb geopotential height patterns over the Northern Hemisphere for a 3-year period, which gives 79.4% variance contribution by the first 10 eigenvectors.

Table 2 lists the average fractional variance Q of the annual and semiannual cycles of those eight parameters after the harmonic analysis at all rectangular grid points. Comparing Tables 1 and 2, it is readily seen that the variance of the first eigenvector of each parameter is largely associated with the annual variation in the data. The harmonic analysis of the principal components of the 700 mb temperature, 300 mb kinetic energy and 300 mb zonal/meridional flow indicator in Table 3 also exemplifies that the variance of the first eigenvectors is mostly dominated by the annual variation.

For the 700 and 500 mb temperature and 700–500 mb thickness which are supposedly respondent to the heating, the first eigenvector contributes 81–82% to the total variance (Table 1). These are less than 94.5% as found by Kidson (1975a) for the first eigenvector of the surface temperature over the Northern Hemisphere, but are overwhelmingly dominant over other components in this study. The first eigenvectors of other parameters in Table 1 which represent the response of the circulation pattern to heating are not as dominant as those of temperature and thickness which are more directly responsive to heating. The kinetic energy and eddy

TABLE 2. Average fractional variance Q (%) of the annual and semiannual cycle.

Parameter	Period of harmonic	
	12 month	6 month
700 mb temperature	84.2	2.1
500 mb temperature	81.9	2.1
700–500 mb thickness	81.4	2.0
300 mb kinetic energy	38.1	6.0
300 mb eddy kinetic energy	35.4	4.1
700 mb zonal/meridional flow indicator	15.2	5.1
500 mb zonal/meridional flow indicator	20.0	4.5
300 mb zonal/meridional flow indicator	23.0	4.7

TABLE 3. Fractional variance Q (%) and phase α (months) in the harmonic analysis of the principal components of 700 mb temperature, 300 mb kinetic energy, and 300 mb zonal/meridional flow indicator. $\alpha = 0$ in mid December and $\alpha = 1$ in mid January.

Eigenvector	Period	700 mb temperature		300 mb kinetic energy		300 mb zonal/meridional flow indicator	
		Q	α	Q	α	Q	α
1	≥2 years	0.4	—	2.0	—	2.7	—
	12 months	98.9	7.4	95.4	1.4	89.7	1.8
	6 months	0.5	1.2	0.3	2.7	0.1	4.1
	4 months	0.0	0.7	0.1	1.6	0.1	1.7
2	≥2 years	17.9	—	8.6	—	4.6	—
	12 months	51.9	10.5	42.7	10.3	8.7	4.7
	6 months	7.5	4.5	30.5	4.3	25.8	1.5
	4 months	2.0	1.8	1.3	1.4	1.0	1.0
3	≥2 years	27.1	—	17.1	—	17.8	—
	12 months	26.1	4.4	4.9	10.0	7.4	5.0
	6 months	28.3	4.4	25.3	1.4	5.4	5.2
	4 months	0.1	0.1	2.6	1.4	0.4	1.1
4	≥2 years	29.3	—	15.4	—	11.8	—
	12 months	5.8	10.0	1.4	10.6	12.1	11.0
	6 months	13.5	4.2	2.2	1.1	22.3	1.0
	4 months	1.9	3.8	1.2	2.6	0.3	2.6
5	≥2 years	50.7	—	11.9	—	11.8	—
	12 months	0.6	10.8	1.4	5.2	24.2	5.2
	6 months	7.1	2.8	2.5	4.2	0.1	3.0
	4 months	1.1	3.8	5.2	1.9	1.6	3.7

kinetic energy have first eigenvectors with variance contributions of 34.7 and 42.9%, respectively. That of the zonal/meridional flow indicator is only 22.1% at 300 mb, and 19.6% and 14.1% at 500 and 700 mb.

The characteristic eigenvector patterns are presented in this paper for the normalized monthly values of the 700 mb temperature, 300 mb kinetic energy and 300 mb zonal/meridional flow indicator. The patterns of 500 mb temperature and 700–500 thickness are similar to those presented patterns of 700 mb temperature. The 300 mb kinetic energy and eddy kinetic energy patterns are also similar. The same is true for patterns of the zonal/meridional flow indicator at the three pressure levels.

Concerning the figures of the eigenvector patterns, except for the first eigenvector of each parameter, the contour interval is 0.04. Because the first eigenvectors have a relatively flat pattern, isopleths are drawn at every 0.005 interval for the temperature series and at every 0.02 interval for the kinetic energy and zonal/meridional flow indicator series. Areas with values > 0.12 are stippled, and areas < -0.12 are cross-hatched with dashed lines. The principal component is shown below the eigenvector pattern.

4. Temperature pattern at 700 mb

The amplitude of the annual cycle in the harmonic analysis as presented in Fig. 1 indicates that most of the annual variation is due to the annual temperature cycle in the mid to high latitudes, whose contour lines are obviously affected by the land-sea configuration. This is reflected in the first eigenvector for the 700 mb temperature (Fig. 2) which accounts for 82.4% of the total variance (Table 1). Large values are located in the mid and high latitudes, particularly over the continents, and the southwestern Pacific and Atlantic contain very low values. Although year-to-year differences can be seen in the summer and winter months, the principal component for the first eigenvector is totally dominated by the annual variation with 98.9% of the fractional variance Q due to the 12-month harmonic (Table 3).

The second eigenvector, although explaining only 3.5% of the total variance (Table 1), clearly shows a land-ocean contrast with large positive values occurring over the oceans and small negative values over the continents (Fig. 3). As shown in Table 3 the principal component has a less regular annual oscillation with 51.9% of Q and with the phase maximum in mid fall. Long-term periods greater than two years account for 17.9% of Q and the semiannual cycle accounts for 7.5% with phase maxima in mid spring and mid fall. A large positive seasonal contribution of this pattern to the deviation from the mean thus occurs in the fall over the low-latitude oceans as also indicated in the principal component shown in Fig. 3. The heating lag of the oceans and heating from increased subsidence due to the anticyclonic intensification in the subtropical oceans during the fall probably account for this.

The third eigenvector as shown in Fig. 4, explaining 2.9% of the total variance (Table 1), has a combined zonal and land-sea contrast with the largest positive values over the lower latitude continents and the largest negative values over the oceans in the higher latitudes. The harmonic analysis of the principal component in Fig. 4 as shown in Table 3 reveals annual and semiannual oscillations of similar magnitude with both cycles having maxima in mid spring. A large positive seasonal contribution to the deviation from the mean thus occurs in spring and smaller negative contributions in mid summer to mid winter as observed in the principal component shown in Fig. 4. The semiannual oscillation in this pattern may reflect the decrease in summer 700 mb temperature due to increased cloudiness over the monsoon region of southern Asia and over Central America. Thus eigenvector 3 of the 700 mb temperature explains much of the variance over the subtropical continents while eigenvector 2 explains much of the variance over the subtropical oceans.

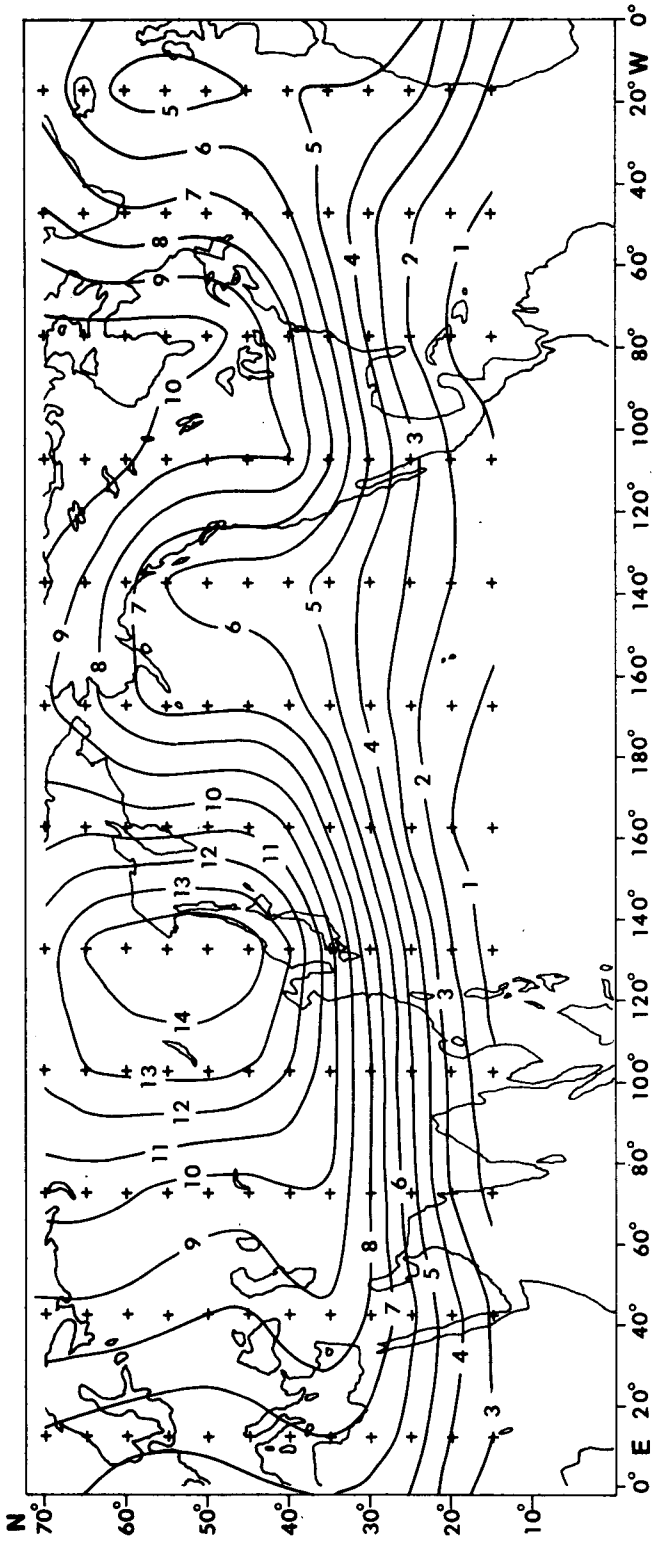

FIG. 1. Amplitude (K) of the annual cycle of the 700 mb temperature for the period 1955–74.

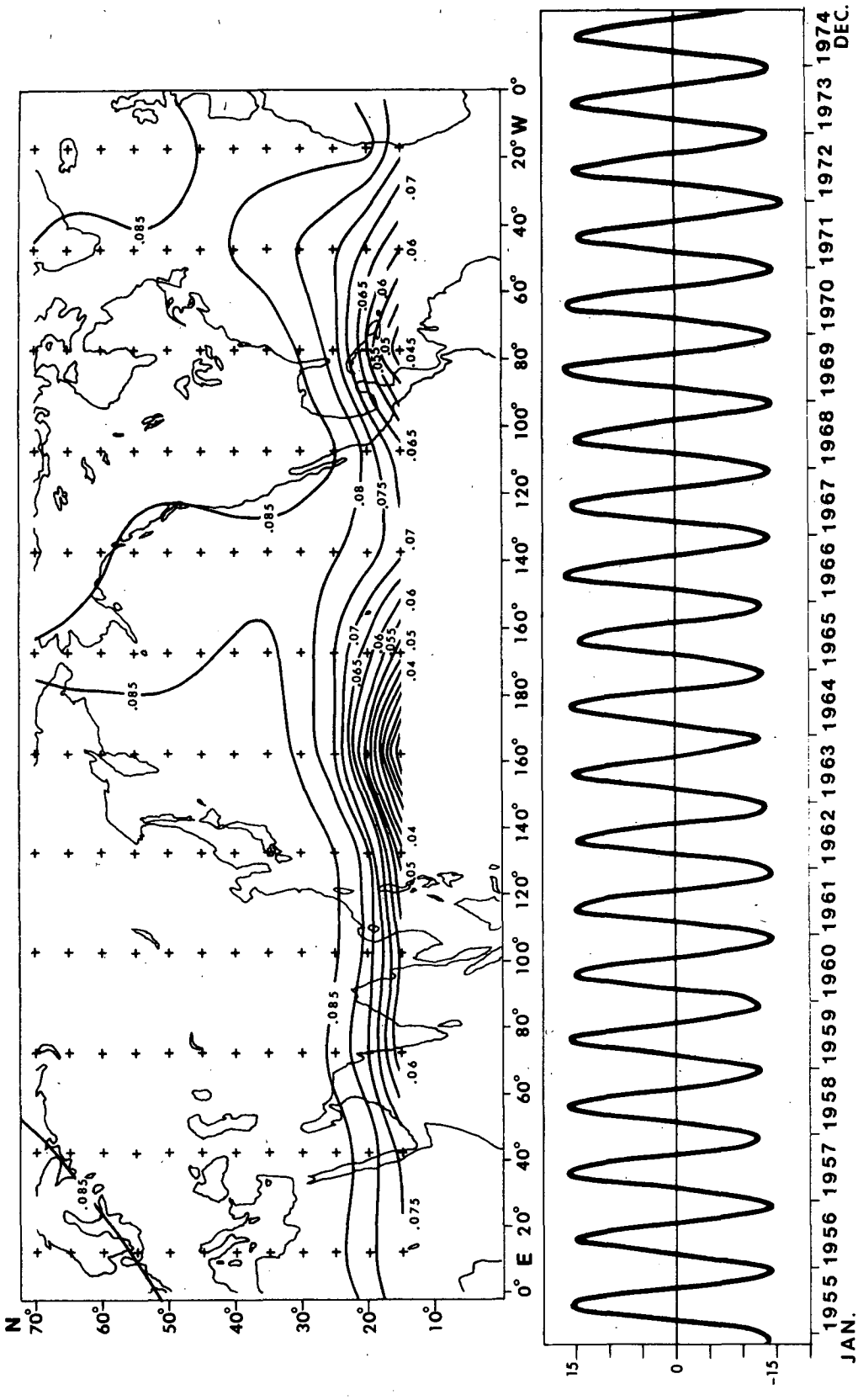

FIG. 2. First eigenvector of the normalized 700 mb temperature and its corresponding principal component for the period 1955–74.

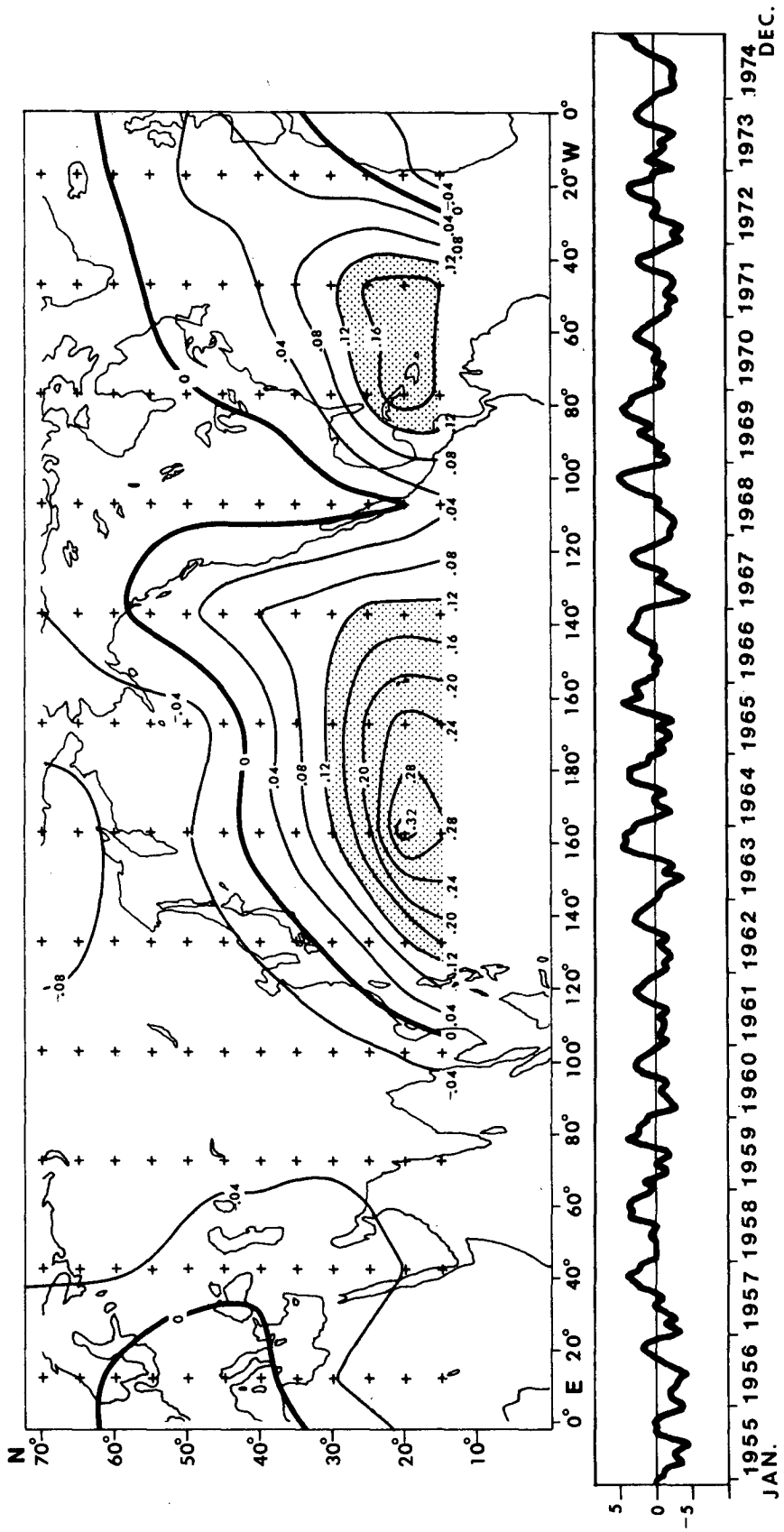

FIG. 3. As in Fig. 2 except for second eigenvector.

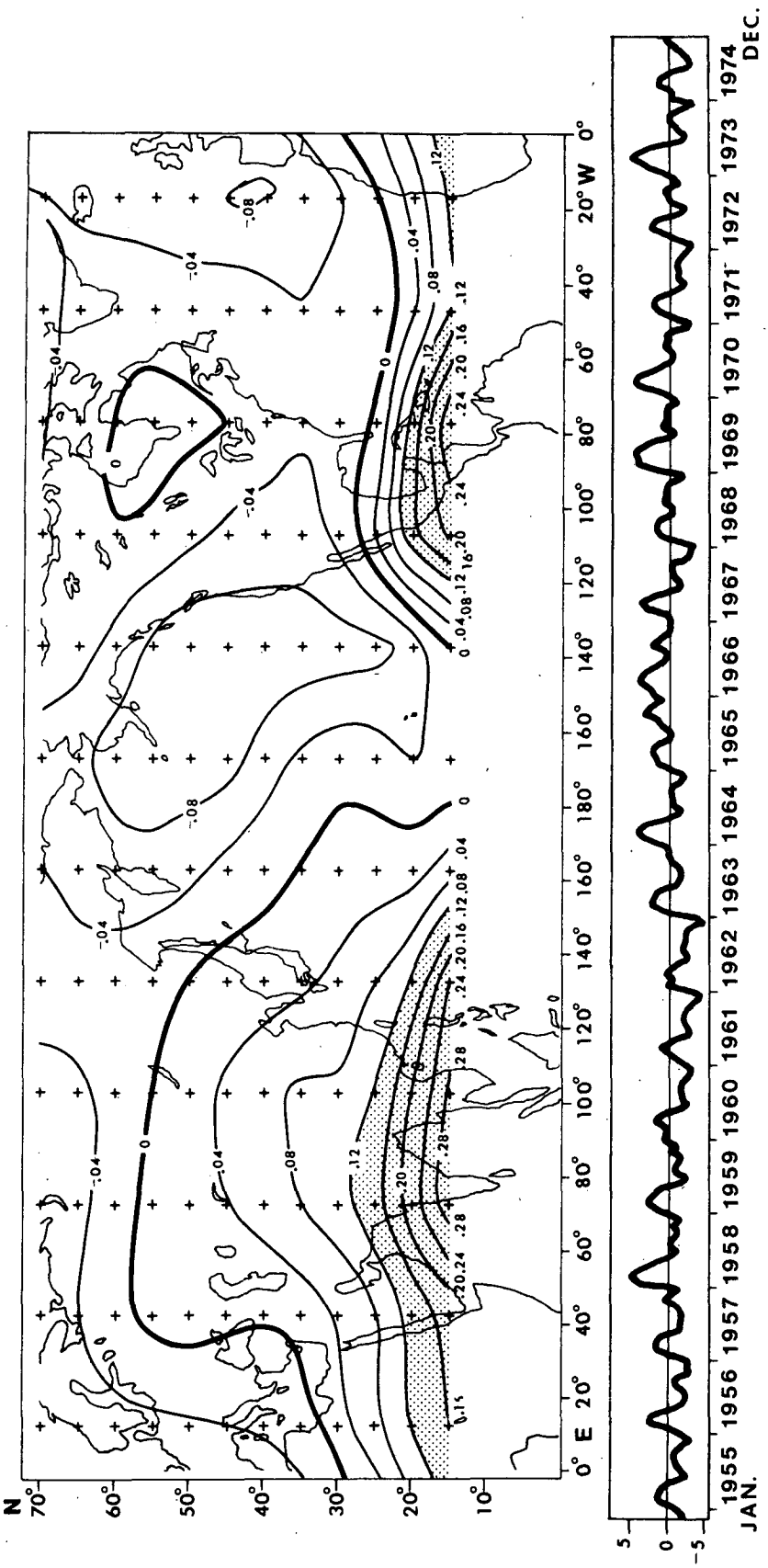

FIG. 4. As in Fig. 2 except for third eigenvector.

Eigenvectors 2 and 3 also seem to involve some long-term variations as well as the regular seasonal variations as shown by the harmonic analysis of the principal component in Table 3. A sharp increase in Q for the long-term variations with periods greater than two years is seen. The significance of the long-term variation may be examined in terms of the latitudinal distribution of the fractional variance in Table 4, in which Q from the harmonic analysis of time series of monthly mean 700 mb temperature at all rectangular grids are averaged zonally at 5° intervals. It is seen in Table 4 that the large Q for the sum of harmonics with periods greater than two years is observed in the lower latitudes while Q for the annual cycle is relatively small in these lower latitudes in comparison with those in middle latitudes. In Table 3 it is also shown that the long-term variations are significant for eigenvectors 4 and 5, whereas the annual cycle becomes negligible for these two eigenvectors. Examination of individual harmonics reveals that the most important contribution to the long-term variation of the 700 mb temperature comes from the southwestern Pacific and southwestern Atlantic. With the maximum data period of 20 years in this study, it will be impossible to resolve the long-term variation. However, as seen in Table 4, the magnitude of the variations with periods longer than 10 years in the lower latitudes stands out significantly.

5. Kinetic energy pattern at 300 mb

The first eigenvector for the 300 mb kinetic energy as shown in Fig. 5 should be approximately determined by the large-scale pattern of the hemispherical circulation. This eigenvector explains 34.7% of the total variance (Table 1), and the harmonic analysis of the principal component in Table 3 shows that the annual cycle dominates this component with 95.4% of Q and the maximum in mid winter. The largest values occur in an extended hemispherical band between 20 and 40°N. The core of the winter jet stream over the southwestern Pacific, eastern North America, China and Northern Africa (see Crutcher, 1959) is generally identified north of the area of the maximum variation. The zonal band of annual variance between 20 and 40°N indicates the latitudinal zone where the annual change of kinetic energy due to the migration of the subtropical jet is significant.

The second eigenvector as shown in Fig. 6, explaining 9.5% of the total variance (Table 1), displays a zonal pattern with large positive values between 50 and 60°N. The principal component has dominant annual and semiannual cycles with 42.7 and 30.5% of Q, respectively (Table 3). The annual cycle has a phase maximum in mid fall and the semiannual cycle has phase maxima in mid fall and mid spring. This results in large positive values during the fall between 50 and 60°N and seems to reflect the shifting of the jet stream from summer to winter.

The third eigenvector, accounting for 6.1% of the total variance, is shown in Fig. 7. The dominant cycle in its principal component is the semiannual cycle with 25.3% of Q and with phase maxima in mid winter and mid summer. The annual cycle in this component is hardly seen although Q from the longer term cycles significantly increases (Table 3). Note the interesting longitudinal variation at 50°N indicating a tendency for the western Pacific and eastern North America to vary out of phase. This could be related to the effect of blocking. The examination of time series at individual rectangular grids which are not shown in the text also indicates that the semiannual cycle dominates in the northwestern Pacific and westward into Eurasia and in

TABLE 4. Fractional variance Q (%) of given sums of harmonics in harmonic analysis of 700 mb temperature for the period 1955–74. H is the number of harmonics included for the specified range of period.

	Period							
Latitude (°N)	20–10 years $H = 2$	6.7–5 years $H = 2$	48–26.7 months $H = 5$	24–12.6 months $H = 10$	12 months $H = 1$	11.4–6.2 months $H = 19$	6 months $H = 1$	5.9–2 months $H = 80$
70	0.4	0.3	0.6	0.7	86.7	1.5	4.4	5.4
65	0.3	0.4	0.7	0.7	87.5	1.6	3.5	5.4
60	0.3	0.4	0.7	0.7	88.1	1.8	2.7	5.3
55	0.2	0.3	0.7	0.8	88.7	1.9	2.1	5.1
50	0.3	0.3	0.6	0.8	89.7	1.8	1.7	4.9
45	0.3	0.3	0.4	0.8	91.7	1.4	1.1	4.1
40	0.4	0.4	0.4	0.8	92.9	1.1	0.8	3.3
35	0.7	0.6	0.4	0.7	92.3	1.3	0.8	3.2
30	0.8	1.0	0.6	0.9	90.3	1.6	1.0	3.8
25	1.5	1.4	1.0	1.1	85.6	2.2	1.5	5.7
20	4.5	4.1	2.7	1.9	70.0	4.3	2.5	10.1
15	11.2	8.4	6.0	3.7	47.3	8.2	2.6	12.6

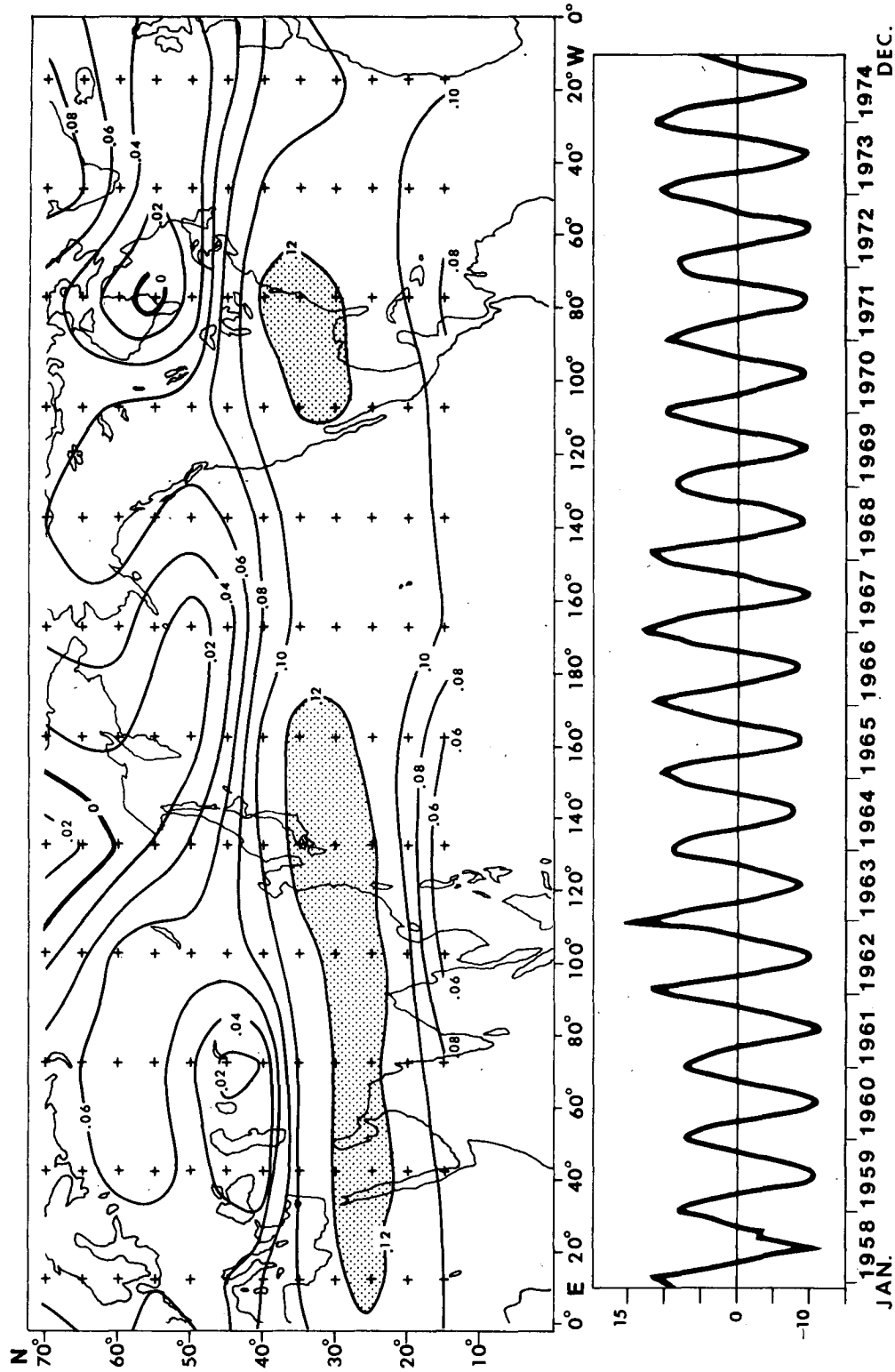

FIG. 5. First eigenvector of the normalized 300 mb kinetic energy and its corresponding principal component for the period 1958–74.

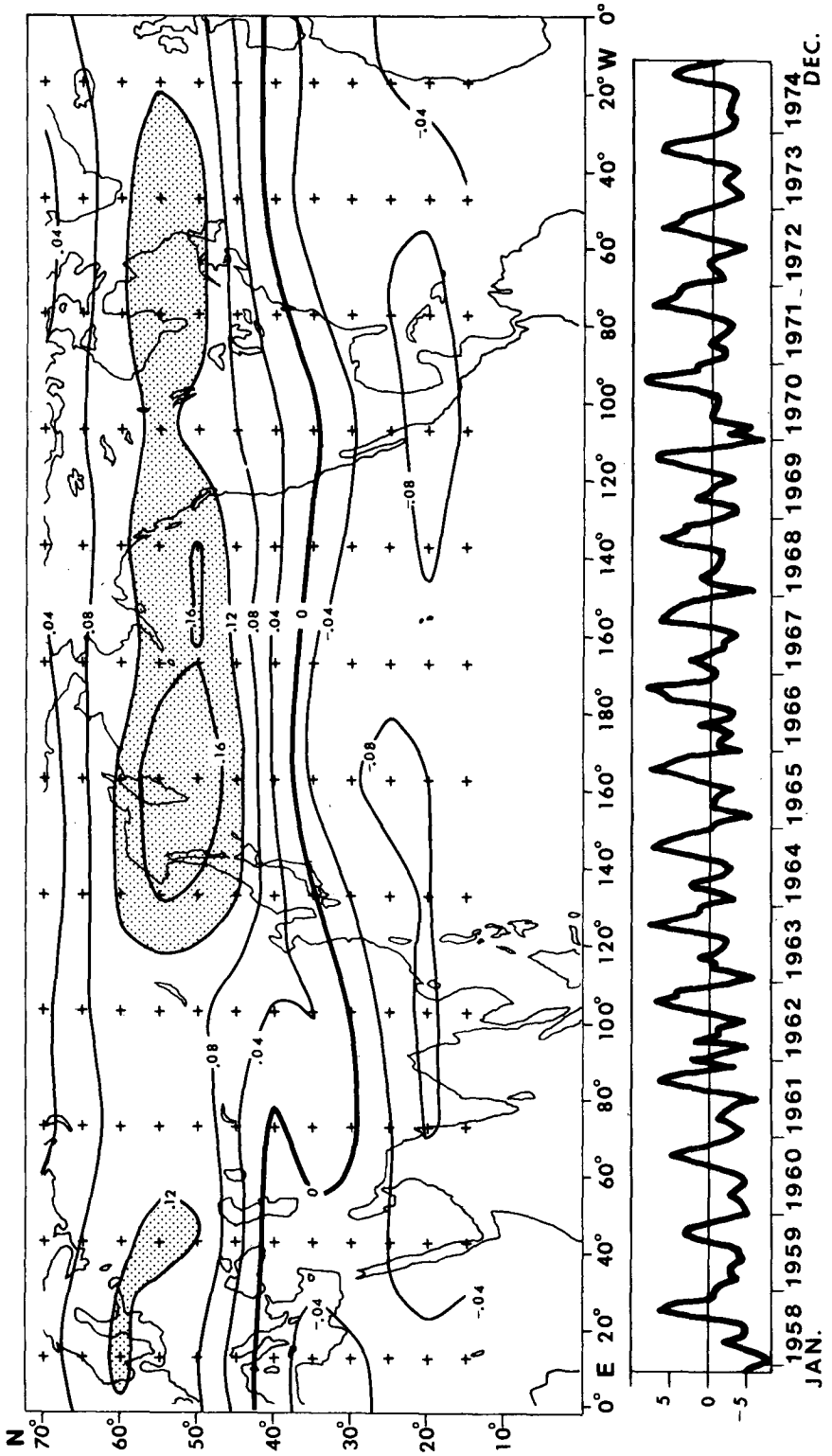

FIG. 6. As in Fig. 5 except for second eigenvector.

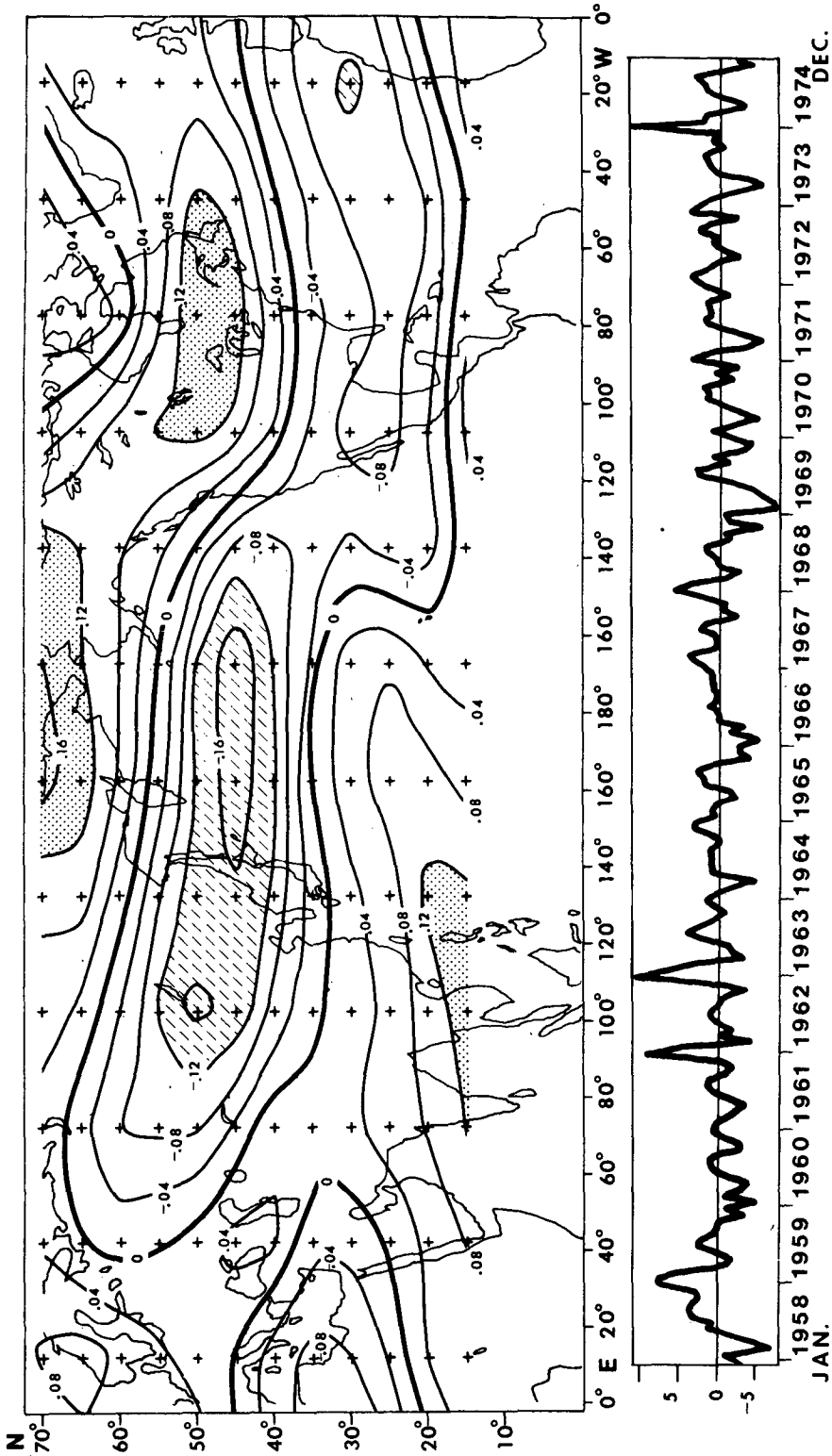

FIG. 7. As in Fig. 5 except for third eigenvector.

southeastern Asia, corresponding to areas as indicated in Fig. 7. This suggests that the third eigenvector of the 300 mb kinetic energy seems to reflect the semiannual oscillation of the wind system such as winter and summer monsoons.

Examination of averaged individual harmonic analyses of the time series over different latitudes in Table 5 indicates that the annual cycle dominates with Q of more than 65% in the subtropical to lower middle latitudes where the effect of the subtropical jet is supposedly maximum, whereas Q for the annual cycle rapidly drops from the middle to higher latitudes. This is in sharp contrast to the Q for the annual cycle of the 700 mb temperature (Table 4) where a dominance of Q with more than 85% variance is seen from 25°N throughout all latitudes poleward. Another interesting feature in Table 5 is the relatively large variances contributed by cycles shorter than one year, whereas those of the 700 mb temperature (Table 4) are essentially insignificant. It is to be noted that Q for the short cycles is particularly pronounced in the middle to higher latitudes where the effects of the annual cycle diminish (Table 5). According to Table 1 the first three eigenvectors of 300 mb kinetic energy account for 50.3% of the total variance, the remainder being distributed among higher number eigenvectors. Accordingly, it may be inferred that the higher number eigenvectors describe the transient patterns in the mid to higher latitudes and the long-term variations which are most observable in the lower latitudes.

6. Zonal/meridional flow indicator

The first eigenvector for the 300 mb zonal/meridional flow indicator shown in Fig. 8 bears a relationship to the subtropical jet and other hemispherical-scale patterns of circulation. Table 3 shows that the annual cycle dominates the principal component associated with the first eigenvector with 89.7% of the fractional variance and has a phase maximum in early February. Areas south of the winter jet maximum have the largest values, which indicate strong zonal flow during winter and relatively weak zonal flow during summer. The second eigenvector pattern in Fig. 9 shows a similar longitudinal variation at 50°N as does the third eigenvector of 300 mb kinetic energy (Fig. 7). This would indicate the tendency for a strong/weak zonal flow over eastern North America and Atlantic at this latitude while a weak/strong zonal flow occurs over the western Pacific. Harmonic analysis of the second principal component in Table 3 shows that the semiannual cycle is the most dominant. It will be pertinent then to associate the second eigenvector of the zonal/meridional flow indicator with the semiannual oscillation of the wind system as was seen with the third eigenvector of the kinetic energy at 300 mb. However, as shown in Table 1, the first and second eigenvectors only contribute 29.2% of the total variance, and the rest of the variance is widely distributed among higher number eigenvectors.

The values of the fractional variance Q in Table 6 show a similar pattern of distribution to that of 300 mb kinetic energy (Table 5). However, Q of the zonal/meridional flow indicator has larger values in the higher frequencies for the mid and higher latitudes. The semiannual cycle of the zonal/meridional flow indicator is also not as obvious as that of the 300 mb kinetic energy. Like other parameters a rather large variance of longer periods in the principal components associated with the third, fourth and fifth eigenvectors is seen in Table 3 with apparent contribution from the lower latitudes (Table 6).

TABLE 5. Fractional variance Q (%) of given sums of harmonics in harmonic analysis of 300 mb total kinetic energy for the period 1958–74. H is the number of harmonics included for the specified range of period.

	Period							
Latitude (°N)	17–8.5 years $H = 2$	5.7–4.3 years $H = 2$	40.8–25.5 months $H = 4$	22.7–12.8 months $H = 8$	12 months $H = 1$	11.3–6.2 months $H = 16$	6 months $H = 1$	5.8–2 months $H = 68$
70	5.4	4.2	3.9	8.4	12.9	12.8	2.3	50.1
65	4.7	3.3	4.7	7.4	15.2	12.7	4.2	47.8
60	3.7	2.2	4.3	6.7	18.8	13.3	7.4	43.4
55	2.9	1.5	4.0	6.5	22.3	11.0	10.9	40.8
50	2.3	1.7	3.9	7.0	21.6	12.1	12.1	39.2
45	2.7	2.3	4.4	8.0	24.9	13.7	9.3	34.7
40	2.8	1.6	4.0	5.7	42.4	11.5	5.2	27.0
35	1.9	0.9	2.0	3.7	66.3	5.9	1.3	18.1
30	1.6	0.9	1.6	2.8	72.2	4.7	3.4	12.8
25	1.3	0.9	2.3	3.2	71.7	4.9	4.8	10.8
20	3.9	1.8	4.0	5.4	57.4	7.8	6.4	13.3
15	9.5	4.8	4.9	9.6	31.9	12.3	4.1	23.0

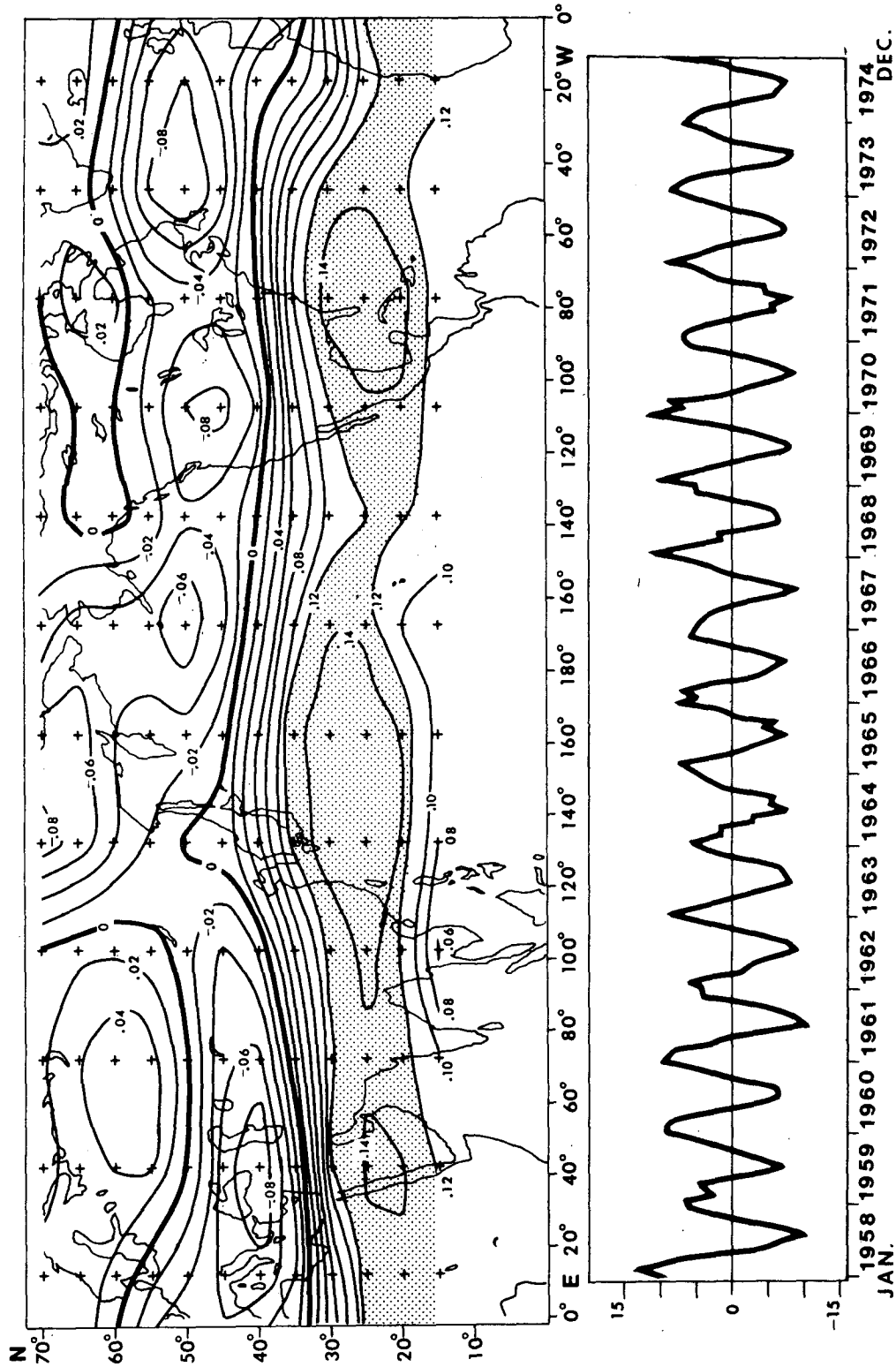

FIG. 8. First eigenvector of the normalized 300 mb zonal/meridional flow indicator and its corresponding principal component for the period 1958–74.

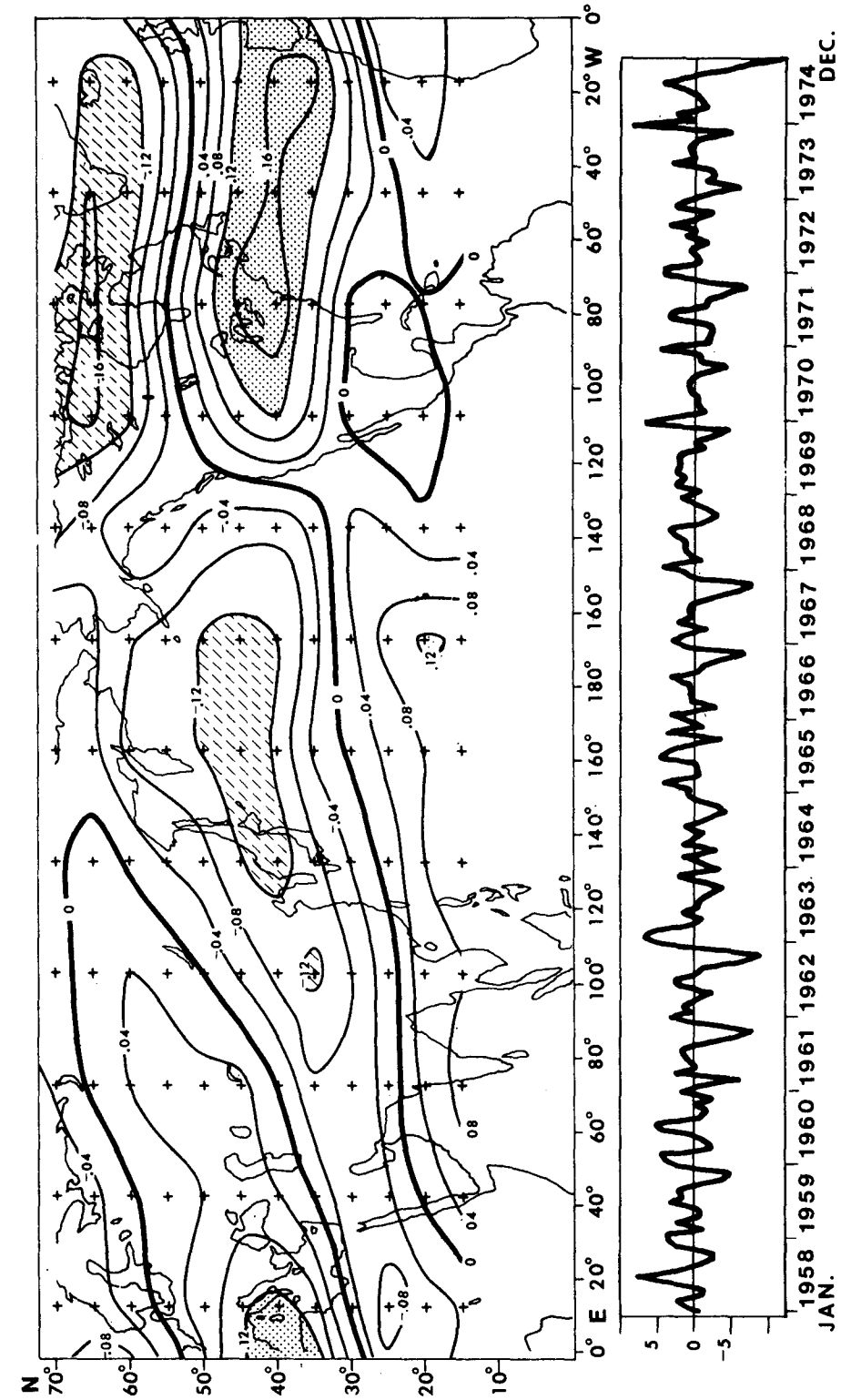

FIG. 9. As in Fig. 8 except for second eigenvector.

TABLE 6. Fractional variance Q (%) of given sums of harmonics in harmonic analysis of 300 mb zonal/meridional flow indicator for the period 1958–74. H is the number of harmonics included for the specified range of period.

Latitude (°N)	Period							
	17–8.5 years $H = 2$	5.7–4.3 years $H = 2$	40.8–25.5 months $H = 4$	22.7–12.8 months $H = 8$	12 months $H = 1$	11.3–6.2 months $H = 16$	6 months $H = 1$	5.8–2 months $H = 68$
70	2.3	2.4	3.7	8.9	4.4	14.6	2.9	60.7
65	1.8	2.5	4.3	8.5	5.0	15.6	4.7	57.5
60	1.9	2.3	5.3	8.7	4.1	17.7	3.9	56.0
55	2.5	2.3	5.6	7.5	7.4	15.2	4.0	55.6
50	3.4	2.8	4.4	8.4	10.4	15.2	3.5	51.9
45	3.6	2.0	3.5	9.0	11.6	16.3	6.7	47.3
40	3.1	1.5	3.1	8.6	12.7	16.3	7.6	47.1
35	2.0	1.8	3.5	7.0	26.7	11.5	3.4	44.1
30	2.6	1.5	3.7	5.1	50.3	7.9	3.0	25.9
25	2.4	1.1	2.6	3.9	61.3	6.2	4.8	17.7
20	4.4	1.2	2.7	6.1	52.3	8.0	7.3	17.9
15	9.5	8.4	4.1	10.1	30.1	11.0	4.2	22.6

7. Concluding remarks

In an attempt to examine the climatological patterns of the upper air circulation in the Northern Hemisphere the eigenvector analysis and harmonic analysis were applied to 20 and 17 years of monthly mean values of temperature, kinetic energy and zonal/meridional flow indicator. It is noted that the first few eigenvectors account for most of the variances of the 700 and 500 mb temperature, and 700–500 thickness patterns with most of the contribution from the first eigenvectors. For the kinetic energy and zonal/meridional flow indicator, however, the first eigenvectors have a much smaller percentage contribution than for those of the temperature fields and more variance is distributed over the higher number eigenvectors. This reflects the close association of the temperature pattern with the large-scale heating field and the more complicated response of the circulation patterns to heating in the space and time domain.

On examination of the eigenvector patterns, associated principal components and harmonics of time series at different latitudes, some distinct features of the Northern Hemispheric circulation become apparent. The first eigenvector of the 700 mb temperature mainly reflects the annual variation of the temperature in the middle and high latitudes with an obvious effect of the land-sea configuration, whereas the second eigenvector of the 700 mb temperature shows a land-ocean contrast. The long-term variation of the 700 mb temperature is large in association with high-numbered eigenvectors over the low-latitude oceans and the variation of the temperature field with periods of 10 years and longer stand out. The first eigenvectors of the 300 mb kinetic energy and zonal/meridional flow indicator are related to the subtropical jet and other hemispherical-scale circulation, which are dominated by the annual cycle. The third eigenvector of 300 mb kinetic energy and second eigenvector of 300 mb zonal/meridional flow indicator appear to reflect the semiannual oscillations of the large-scale wind systems including summer and winter monsoons. The higher number eigenvectors of the kinetic energy and zonal/meridional flow indicator appear to be associated with the short-term variations of transient circulations in the mid to high latitudes and also with long-term variations which are most observable in the lower latitudes.

Acknowledgments. The authors gratefully acknowledge the assistance of H. A. Burgdorf and D. M. Botner during the course of study. Technical assistance rendered by C. W. Irwin, Juliana Lee, Mary Robertson, Dawn Stringfield and Betty Whitmarsh is also sincerely acknowledged.

Special thanks are due to Mr. A. F. Krueger for his valuable comments concerning the physical interpretation of eigenvectors.

REFERENCES

Craddock, J. M., and C. R. Flood, 1969: Eigenvectors for representing the 500 mb geopotential surface over the Northern Hemisphere. *Quart. J. Roy. Meteor. Soc.*, **95**, 576–593.

Cressman, G. P., 1959: An operational objective analysis system. *Mon. Wea. Rev.*, **87**, 367–371.

Crutcher, H. L., 1959: Upper wind statistics charts of the Northern Hemisphere, Vol. II. Office of the Chief of Naval Operations, NAVAER 50-1C-535. [Library of Congress Document No. G1050.C7, 1959, Map].

Gray, T. I., J. R. Irwin, A. F. Krueger and M. S. Varnadore, 1976: Average circulation in the troposphere over the tropics. S/T 76-1756, NOAA, U.S. Dept. of Commerce, 218 pp. [Govt. Printing Office, Stock No. 003-017-0037-05-2].

Kidson, J. W., 1975a: Eigenvector analysis of monthly mean surface data. *Mon. Wea. Rev.*, **103**, 177–186.

——, 1975b: Tropical eigenvector analysis and the southern oscillation. *Mon. Wea. Rev.*, **103**, 187–196.

Kung, E. C., 1977: Energy sources in middle-latitude synoptic-scale disturbances. *J. Atmos. Sci.*, **34,** 1352–1365.

——, and S. Soong, 1969: Seasonal variation of kinetic energy in the atmosphere. *Quart. J. Roy. Meteor. Soc.*, **95,** 501–512.

Kutzbach, J. E., 1967: Empirical eigenvectors of sea-level pressure, surface temperature and precipitation complexes over North America. *J. Appl. Meteor.*, **6,** 791–802.

——, 1970: Large-scale features of monthly mean Northern Hemisphere anomaly maps of sea-level pressure. *Mon. Wea. Rev.*, **98,** 708–716.

Oort, A. H., and E. M. Rasmusson, 1971: Atmospheric circulation statistics. NOAA Professional Paper 5, U.S. Dept. of Commerce, 323 pp. [Govt. Printing Office, Stock No. 0317-0045].

Rinne, J., 1971: Investigation of the forecasting error of a simple barotropic model with the aid of empirical orthogonal functions. Parts I and II. *Geophysica*, **11,** 185–239.

Stidd, C. K., 1967: The use of eigenvectors for climatic estimates. *J. Appl. Meteor.*, **6,** 255–264.

Trenberth, K. E., 1975: A quasi-biennial standing wave in the Southern Hemisphere and interrelations with sea surface temperature. *Quart. J. Roy. Meteor. Soc.*, **101,** 55–74.

Wahl, E. W., 1972: Climatological studies of the large-scale circulation in the Northern Hemisphere. *Mon. Wea. Rev.*, **100,** 553–564.

Weare, B. C., 1977: Empirical orthogonal analysis of Atlantic Ocean surface temperature. *Quart. J. Roy. Meteor. Soc.*, **103,** 467–478.